

CFD Simulation of Two Phase Leak Flow Through Circular and Rectangular Circumferential Cracks from High Pressure High Temperature Pipelines

Anwar Hussain¹; Sandip Ghosh²

^{1,2}Department of Mechanical Engineering, JIS College of Engineering, Kalyani, India

Publication Date: 2025/06/30

Abstract: Leak flow prediction has become a part and parcel of safe design in high pressure high temperature piping systems. This study investigates the behavior of mass flux, flow velocity and phasic transformation through circumferential cracks with circular and rectangular geometries from high-pressure high temperature pipelines. 3-dimensional computational hydrodynamic simulations were performed to model narrow leaks simulating the conditions of a pressurized water reactor. The simulations examined variations in mass flux and velocity for different crack sizes under a stagnation pressure range of 70 to 100 bar. Results demonstrate that both mass flux and velocity consistently increase with pressure. For circular cracks, mass flux increased by up to 20.2%, while average velocity rose by 20%. In smaller cracks, the increases in mass flux and velocity were around 19.8%. Rectangular cracks exhibited similar trends, with mass flux increasing by up to 19.6% and velocity by 19.7%. These findings demonstrate the strong dependence of leakage behavior on both pressure and crack geometry, which is critical for predicting failure risks in high-pressure systems.

Keywords: Leak, Pipe, Crack, High pressure High temperature, Multiphase.

How to Cite: Anwar Hussain; Sandip Ghosh; (2025) CFD Simulation of Two Phase Leak Flow Through Circular and Rectangular Circumferential Cracks from High Pressure High Temperature Pipelines. International Journal of Innovative Science and Research Technology, 10(6), 2159-2165. <https://doi.org/10.38124/ijisrt/25jun1623>

I. INTRODUCTION

The transportation of fluid materials through piping systems is one of the most convenient and economical whether it involves supplying potable water to a city, transporting materials in industries or disposing of waste fluids. However, the occurrence of cracks in the piping system can disrupt its intended performance leading to economic losses as well as environmental and public health concerns. The unintentional formation of cracks is often inevitable due to factors such as inherent defects, use of unsuitable pipe materials, poor workmanship, inadequate design considerations or poor maintenance planning or some unforeseen reasons. Understanding the flow characteristics crucial for expected system performance. The experimental and numerical investigations performed by Ali et. al.[2] with three different shapes of crack geometries circular, square and slot shaped to examine pressure and velocity distributions revealed that the magnitude of pressure and velocity swiftly alter near the leak location and the pressure is found higher at upstream than downstream due to presence of crack. Shao et.al.[14] through their experimental study compared the discharge from orifices of different shapes; circular, circumferential and longitudinal and

reported that the discharge from the longitudinal orifice has least sensitivity when the orifice pressures and opening areas were identical. Sousa et. al [3] observed the influence of leakage of oil on pressure and flow rate characteristics in pipelines and focused on pressure and velocity fields as essential factors for identifying leaks in pipelines. Research on small-scale leaks by Mansour et.al [4] in water pipelines has also employed CFD methods to evaluate the influence of low-pressure variations on leakage characteristics. Kanan et.al [5] has shown that the modified two-parameter fracture criterion is effective in distinguishing between leak and break cases and this allows taking necessary precautions in advance and provides a useful tool for designers. Further investigations into leak dynamics include Heckmann et al. [6], who emphasized the need to estimate leak flow rates due to their effect on system performance. Silva et al. [7] assessed three different materials under Leak-Before-Break (LBB) scenarios, concluding that all exhibited plastic failure modes while satisfying the established performance limits. Dubyk [8] used a probabilistic LBB analysis via the Failure Assessment Diagram (FAD), demonstrating that crack morphology and fracture toughness significantly influence leak rate, with the latter having a stronger effect than yield strength. Fatigue behavior and crack propagation have also

been studied using damage tolerance principles. Kebir et al. [9] provided insights into enhancing pipeline durability and structural integrity. Jafar et al. [10] identified changes in fluid viscosity near the crack, which further influences local flow behavior. Among the variety of works reported in literature, the leak flow data for high pressure scenarios especially in presence of high temperature is quite a few and also belongs to narrow ranges of pressure. In the present work, the computational simulations have been performed to explore the effect of varying range of pressure, crack type and crack shape on single and two phase leakages.

II. PHYSICAL PROBLEM

A. Modelling of the computational domain

In the present work, a study has been conducted using a 100 NB pipe of 100 mm & 300 mm length respectively for single phase and multiphase simulations. Three dimensional mode of pipe with circumferential cracks or slits have been developed for the simulation. Normal water and its standard properties are considered as the fluid under leak flow condition and wall conditions are designated with

the properties of carbon steel. The major flow diameter was taken as 100 mm with a pressure gradient of 1 bar between the inlet and outlet for all crack dimensions. Rectangular cracks of sizes 1mm x 2mm, 1mm x 5mm, and 1mm x 8mm and circular cracks of diameters 1mm, 3mm, and 5mm were created. Inlet pressures were taken as 70, 80, 90 and 100 bar. Pressure selected in the range of PWR reactor primary loop pressure range. Cracks have been generated in an open source CFD simulation platform in the similar way. Mesh generation and refinement was conducted by adjusting parameters such as element size and number of divisions while validating computational setup. Discretization is achieved through the appropriate model selections as referred by allied researchers. Mass flow rate was determined by solving continuity and momentum equation using CFD code and appropriate turbulence model. Standard K-epsilon model was considered for the present analysis with different pressure inlet values and a constant pressure gradient for different crack dimensions. The data has been used to compute mass flow rate (Kg/s) and velocities at crack outlets for analysis. The details of the geometrical of the test section have been depicted in Figure 1.

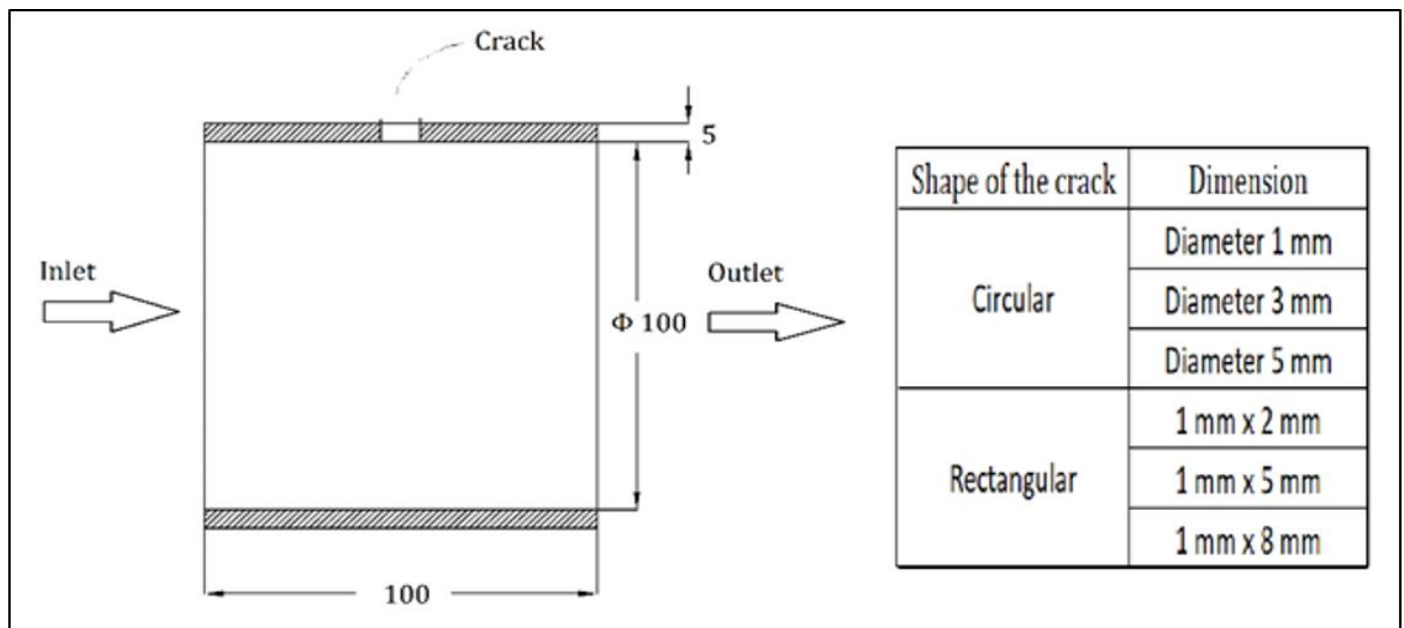


Fig 1 Cross sectional details of the geometry

B. Mesh Independence test

The following simulations have been performed for different mesh elements to determine the appropriate mesh configuration.

Table 1 Data for mesh Independence

Mesh	Inlet pressure (Bar)	Crack diameter (m)	Mass flux through crack (Kg/m ² s)	Average velocity (m/s) at [Crack]
111871	70	0.005	8.87E+04	87.06217
167824	70	0.005	8.77E+04	85.78396
252535	70	0.005	8.81E+04	86.17564
379681	70	0.005	8.87E+04	87.04682
571439	70	0.005	8.80E+04	86.18799
857373	70	0.005	8.84E+04	86.60603
948622	70	0.005	8.81E+04	86.29964
From Richardson		8.78E+04	86.20957	Extrapolation

The data indicates as shown in Table 1 strong evidence of mesh convergence in the simulation results. With a constant inlet pressure of 70 bar and a fixed crack diameter of 0.005 meters, both the mass flux and average velocity at the crack show minimal variation across progressively refined meshes. The mass flux ranges narrowly between 87,700 and 88,700 kg/m²·s, while the average velocity fluctuates between 85.78 and 87.06 m/s. These small differences suggest that the solution is approaching mesh independence. Three mesh configurations have been considered from these such that grid refinement ratio is 1.5 which is in accordance with the minimum value of 1.3 as recommended by Roache [11]. The values obtained through Richardson extrapolation (87,800 kg/m²·s for mass flux and 86.21 m/s for velocity) fall well within the observed range, further confirming the validity of the numerical results. Overall, the simulation demonstrates consistent and stable behaviour as the mesh is refined and further increases in mesh density are unlikely to produce significant improvements in accuracy. Finest mesh of 948622 and higher elements is chosen for the final simulations.

C. Boundary conditions

A pressure-based standard k-epsilon turbulence model has been employed in the simulation, utilizing double precision. The inlet pressure has been adjusted while maintaining a constant outlet pressure through a crack. The outlet pipe pressure has been set to uphold a consistent pressure gradient for the primary pipe flow. The Reynolds number has been calculated for the flow regime and found to be in the range of Re≈4378-5000, which is more than 4000 that suggests it is turbulent flow following the previous work reported in the literatures. The K-ε model has ability of prediction (extrapolation) as reported in literature like Sun et.al., [12]. Nunes Sousa et.al. [13] used homogeneous model for turbulence as K-ε model in their work. Ogunesan et.al [14], in their study they found that RNG K-epsilon model to be precise and it can be relied for broader types of flows. The governing equations for describing the flow of fluid in the pipe and leakage entail the conservation of mass and momentum. The fluid properties are considered Newtonian and incompressible, with constant physical and chemical attributes. Moreover, the flow is assumed to be three-dimensional and isothermal. The specific equations characterizing the flow are delineated below.

$$\frac{\partial}{\partial t}(\rho_m \vec{v}_m) + \nabla \cdot (\rho_m \vec{v}_m \vec{v}_m) = -\nabla_p + \nabla \cdot [\mu_m (\nabla \vec{v}_m + \nabla \vec{v}_m^T)] + \rho_m \vec{g} + \vec{F}_+ + \nabla \cdot (\sum_{k=1}^n \alpha_k \rho_k \vec{v}_{dr,k}) \tag{7}$$

Where *n* is the number of phases, \vec{F} is a body force, and μ_m is the viscosity of the mixture:

$$\mu_m = \sum_{k=1} \alpha_k \mu_k \tag{8}$$

$v_{dr,k}$ is the drift velocity for secondary phase k:

For single phase analysis, the equation for momentum conservation in the direction of i can be expressed as-

$$\frac{\delta}{\delta t}(\rho \bar{U}_i) + \frac{\delta}{\delta x_j}(\rho U_i U_j) = -\frac{\delta p}{\delta x_i} + \frac{\delta}{\delta x_j} \left(\mu \frac{\delta U_i}{\delta x_j} \right) \tag{1}$$

The continuity equation exhibits the following form at the leak location:

$$Q_{up} - Q_{down} - Q_{leak} = 0 \tag{2}$$

Where, Q_{up} and Q_{down} is the discharge in the upstream and the downstream of leak location respectively. Q_{leak} is the flow rate of the leak. Pressure drop across the test section is determined by the Darcy-Weisbach equation –

$$\Delta P = L \times f_D \times (\rho / 2) \times (v^2 / D) \tag{3}$$

where, L = the length of the pipe [m], D = pipe diameter in m, Δp = pressure loss [Pa], ρ = fluid density [kg/m³], f_D = Darcy friction factor, v = mean fluid velocity [m/s], friction factor $f_D = 64 / Re$, where Re is Reynolds number.

For multiphase flow simulation the following equations were considered under a mixture model,

The continuity equation for the mixture is

$$\frac{\partial}{\partial t}(\rho_m) + \nabla \cdot (\rho_m \vec{v}_m) = 0 \tag{4}$$

Where \vec{v}_m is the mass-averaged velocity:

$$\vec{v}_m = \frac{\sum_{k=1}^n \alpha_k \vec{v}_k}{\rho_m} \tag{5}$$

And ρ_m is the mixture density:

$$\rho_m = \sum_{k=1}^n \alpha_k \rho_k \tag{6}$$

α_k is the volume fraction of phase k.

The momentum equation for the mixture can be obtained by summing the individual momentum equations for all phases. It can be expressed as

$$\vec{v}_{dr,k} = \vec{v}_k - \vec{v}_m \tag{9}$$

The energy equation for the mixture takes the following form:

$$\frac{\partial}{\partial t} \sum_{k=1}^n (\alpha_k \rho_k E_k) + \nabla \cdot \sum_{k=1}^n (\alpha_k \vec{v}_k (\rho_k E_k + P)) = \nabla \cdot k_{eff} \nabla T + S_E \tag{10}$$

Where k_{eff} is the effective conductivity $\sum \alpha_k (k_k + k_t)$, where k_t is the turbulent thermal conductivity, defined according to the turbulence model being used. The first term on the right-hand side of Equation 10 represents energy transfer due to conduction. S_E includes any other volumetric heat sources.

III. RESULT AND DISCUSSION

➤ *Flow prediction for Single phase simulation*

Table 2 Mass flux and maximum leak flow velocity data predicted for circular cracks

Inlet pressure (Bar)	Crack diameter (m)	Crack opening area (COA) (m ²)	Discharge through crack (Kg/s)	Average velocity (m/s)
70	0.005	19.6E-06	1.7790	1.00E+02
80	0.005	19.6E-06	1.9074	1.08E+02
90	0.005	19.6E-06	2.0276	1.14E+02
100	0.005	19.6E-06	2.1410	1.21E+02
70	0.003	7.07E-06	0.6490	9.41E+01
80	0.003	7.07E-06	0.6954	1.01E+02
90	0.003	7.07E-06	0.7390	1.07E+02
100	0.003	7.07E-06	0.7801	1.13E+02
70	0.001	0.78E-06	0.0683	9.09E+01
80	0.001	0.78E-06	0.0732	9.74E+01
90	0.001	0.78E-06	0.0777	1.03E+02
100	0.001	0.78E-06	0.0820	1.09E+02

For circular cracks the predicted mass flux and maximum leak flow velocity has been depicted in Table 2. The results have been demonstrated for 70 bar, 80 bar, 90 bar and 100 bar inlet pressure conditions. For each pressure leak flow simulation has been observed for 3 sets of crack

opening areas. Similarly, for rectangular cracks all such pressure conditions were simulated through the CFD module using applicable boundary conditions. The results have been shown in table 3.

Table 3 Mass flux and maximum leak flow velocity predicted for rectangular cracks

Inlet pressure (Bar)	Crack dimension Rectangular (m x m)	Crack opening area (COA) (m ²)	Discharge through crack (Kg/s)	Average velocity (m/s)
70	0.001 x 0.008	8.00E-06	0.0259	2.62E+03
80		8.00E-06	0.0277	2.81E+03
90		8.00E-06	0.0295	2.98E+03
100		8.00E-06	0.0311	3.14E+03
70	0.001 x 0.005	5.00E-06	0.0161	2.61E+03
80		5.00E-06	0.0172	2.79E+03
90		5.00E-06	0.0183	2.96E+03
100		5.00E-06	0.0193	3.13E+03
70	0.001 x 0.002	2.00E-06	0.0063	2.57E+03
80		2.00E-06	0.0068	2.75E+03
90		2.00E-06	0.0072	2.92E+03
100		2.00E-06	0.0076	3.08E+03

The variation of discharge and velocity with respect to inlet pressure and crack opening area (COA) for both circular and rectangular cracks is illustrated in Figures 2 to 9. For circular cracks, Figures 2 and 3 show that both

discharge and velocity increase with inlet pressure across all crack diameters. As seen in Table 2, at a constant crack size, the discharge rises nearly linearly with pressure. For example, at a 5 mm diameter (COA = 19.6 × 10⁻⁶ m²), the

discharge increases from 1.7790 kg/s at 70 bar to 2.1410 kg/s at 100 bar. Corresponding velocity increases from 100 m/s to 121 m/s, indicating a steady rise in flow speed with pressure. Figures 4 and 5 further illustrate that both discharge and velocity also increase with COA at a given

pressure. The discharge response is particularly sensitive to COA, reflecting the proportionality between flow rate and available flow area. However, the velocity increases more moderately, suggesting that pressure is the dominant driver of flow speed while COA governs the total mass throughput.

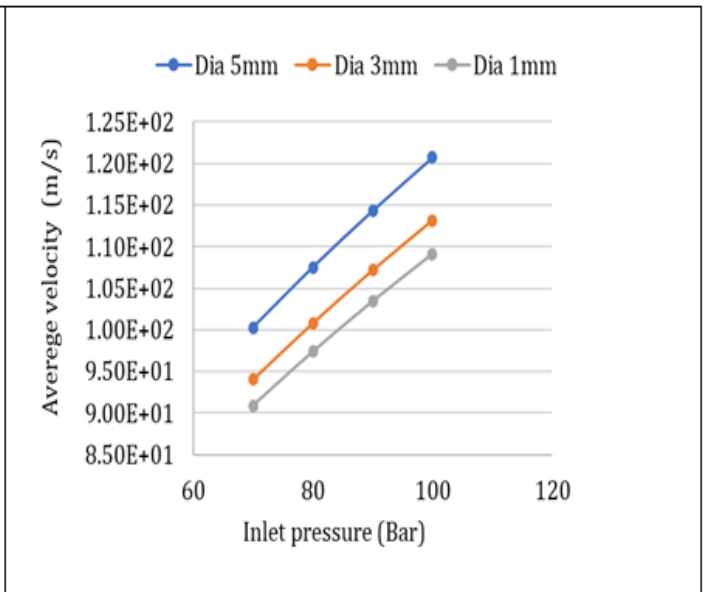
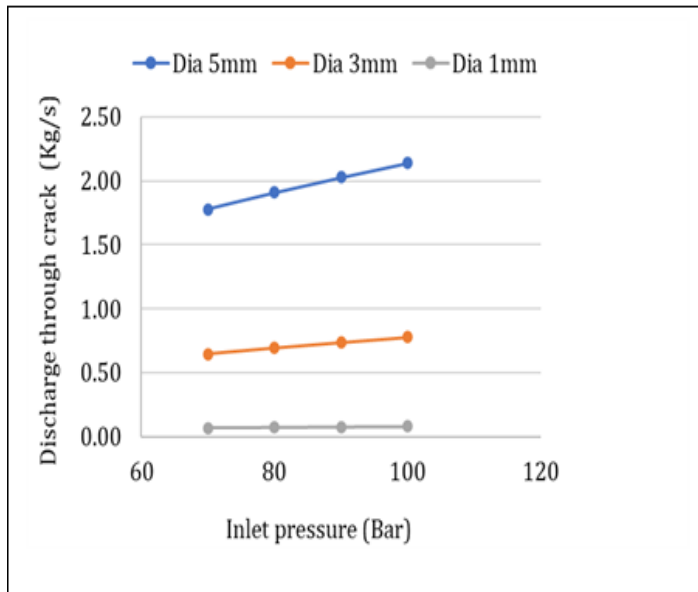


Fig 2 Discharge variance with inlet pressure (Circular)

Fig 3 Velocity variance with inlet pressure (Circular)

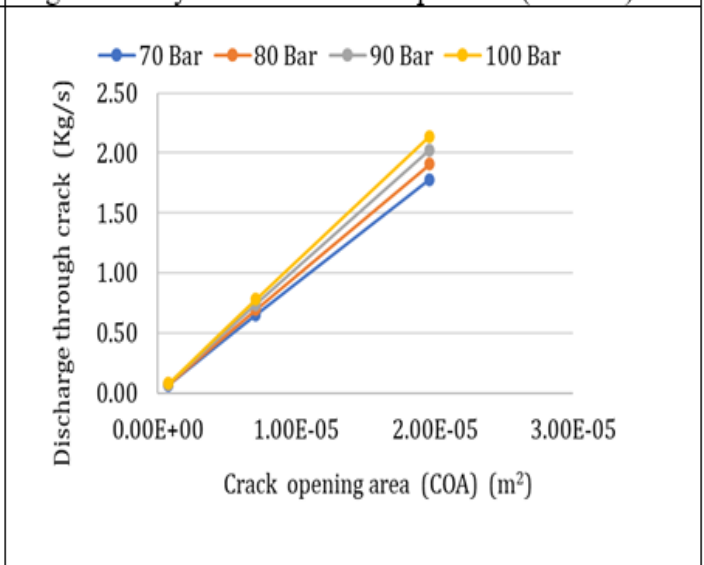
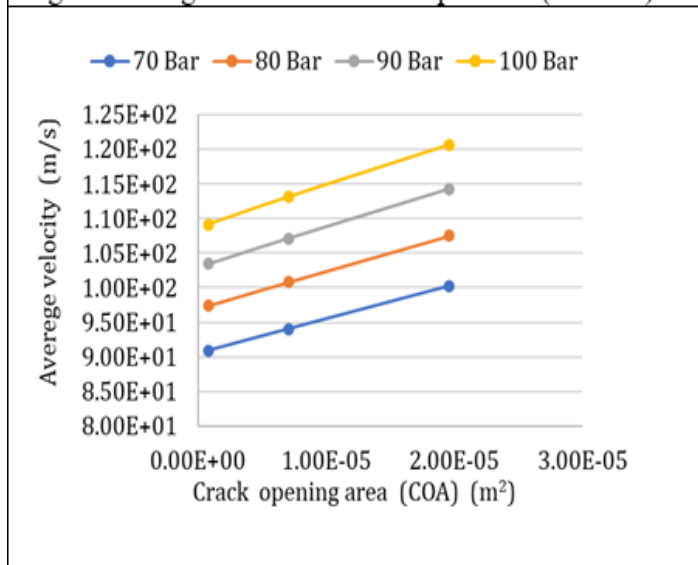


Fig 4 Velocity variance with COA (Circular)

Fig 5 Discharge variance with COA (Circular)

In the case of rectangular cracks, similar trends are observed. Figures 6 and 7 show a consistent increase in discharge and velocity with inlet pressure across all crack dimensions. Table 3 indicates that for the largest rectangular crack (1 mm × 8 mm, COA = 8.00 × 10⁻⁶ m²), the discharge increases from 0.0259 kg/s at 70 bar to 0.0311 kg/s at 100 bar, while velocity increases from 2.62 × 10³ m/s to 3.14 × 10³ m/s. Notably, rectangular cracks exhibit significantly higher velocities than circular ones, even at smaller COAs, due to their narrow width and elongated geometry, which accelerate the fluid more intensely. Figures 8 and 9 confirm that both discharge and velocity scale with COA, with velocity increasing more subtly compared to the strong rise

in discharge. Overall, the results from both geometries demonstrate that inlet pressure primarily influences velocity, while crack opening area has a more significant impact on discharge. The flow trends are consistent with theoretical expectations for compressible flow through small openings and support the use of power-law relationships for modeling these behaviours.

• *Quantitative Analysis of the Trends*

To quantify the relationship between inlet pressure with mass flux and velocity for different crack geometries, regression was performed on the simulation data.

Table 4 Trend fitting and R² values

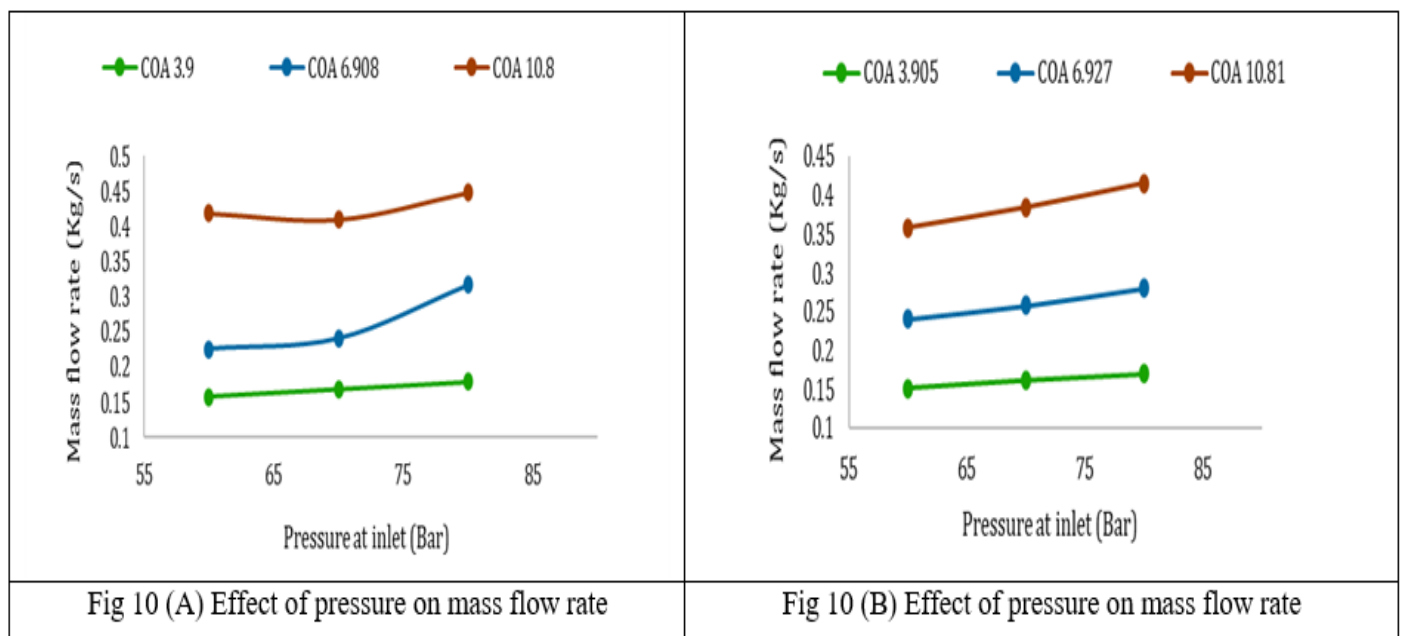
Shape	Crack dimension	Parameter	Equation (Power - law)	R ²	Legend
Circular	Dia 1mm	Mass flux	$y = 0.0078x^{0.5119}$	1	y = Discharge, x = Inlet pressure
Circular	Dia 3mm	Mass flux	$y = 0.0726x^{0.5156}$	1	
Circular	Dia 5mm	Mass flux	$y = 0.1959x^{0.5193}$	1	
Circular	Dia 1mm	Velocity	$y = 10.335x^{0.5119}$	1	y = Velocity, x = Inlet pressure
Circular	Dia 3mm	Velocity	$y = 10.414x^{0.518}$	1	
Circular	Dia 5mm	Velocity	$y = 10.976x^{0.5207}$	1	
Rectangular	1mm x 2mm	Mass flux	$y = 0.0007x^{0.5109}$	1	y = Discharge, x = Inlet pressure
Rectangular	1mm x 5mm	Mass flux	$y = 0.0019x^{0.5089}$	1	
Rectangular	1mm x 8mm	Mass flux	$y = 0.003x^{0.5113}$	1	
Rectangular	1mm x 2mm	Velocity	$y = 293.73x^{0.5106}$	1	y = Velocity, x = Inlet pressure
Rectangular	1mm x 5mm	Velocity	$y = 298.71x^{0.5098}$	1	
Rectangular	1mm x 8mm	Velocity	$y = 301.21x^{0.5093}$	1	

The CFD data indicate a consistent power-law relationship between inlet pressure and both mass flux and velocity across different crack shapes and dimensions. As depicted in Table 4. For all cases, the equations exhibit an excellent fit with an R² value of 1, suggesting highly reliable correlations. The exponents across all datasets are approximately 0.51, reflecting a square-root dependence on pressure. In circular cracks, mass flux increases significantly with diameter, aligning with the expected increase in flow area (proportional to the square of the diameter). However, the velocity shows only a modest rise with diameter, indicating that the increased discharge is primarily area-driven. In contrast, rectangular cracks show a linear increase in mass flux while velocity remains relatively high and stable across all sizes. Overall, the results demonstrate that while both mass flux and velocity follow similar pressure

dependencies, their magnitudes are strongly influenced by crack geometry and size. The power-law models derived are robust and suitable for predictive analysis of flow through cracks under varying pressure conditions.

➤ *Flow prediction for multiphase simulation*

Figure 10 (a), (b) shows the mass flow rate through the cracks of different shapes and sizes for rectangular and circular cracks respectively. The mass flow rate is found positively correlated with pressure that is mass flow rate increases with increase in inlet pressure, which shows a similar trend with other researchers like Manna et.al., (2023). At lower subcooling, Revanker et.al., (2013) have found that the mass flux increases due to lower rate of vaporization. Larger cracks tend to exhibit greater sensitivity to pressure changes.



Effect of pressure on vapor volume fraction has been shown in Figure 11 (a) and (b) for various shapes of the crack, there is a general trend that vapor volume fraction increases with increasing size of the crack which shows that

there are less non equilibrium effects with greater crack opening area. The finding is comparable with the experimental outcomes available in literatures such as Amos et.al., [15].

IV. CONCLUSION

A comprehensive computational study was conducted to predict flow characteristics through predefined cracks under high-pressure and high-temperature conditions, representative of primary circuits in nuclear power plants. Discharge and velocity through cracks are strongly influenced by inlet pressure and crack opening area (COA) with consistent trends observed across both circular and rectangular geometries. Discharge increases nearly linearly with pressure, while velocity also rises, though more moderately, indicating that pressure primarily drives flow acceleration, while COA governs total mass flux. Rectangular cracks exhibit significantly higher velocities than circular ones even at lower COAs. Overall, crack shape plays a critical role in flow characteristics, with rectangular geometries favoring higher-speed jets, whereas circular ones yield higher discharge for the same COA. The HPHT multiphase flow analysis demonstrated the influence of pressure and the crack geometry on mass flow rate and vapor volume fraction at crack exit plane. The results indicate that sudden depressurization near the crack zone leads to formation of vapor with mass flux increasing almost linearly with inlet pressure at a fixed subcooling level. These findings align closely with prior research data in this field.

REFERENCES

- [1]. Amos C. N. and Schrock V. E., Critical discharge of initially subcooled water through slits, USNRC; NUREG-CRe3475 (1983).
- [2]. Ali J. A. and Ahmed P., Flow characteristics around the crack in pipeline, *J. Phys.: Conf. Ser.*, vol. 2594, 012023, (2023).
- [3]. Ali S., Hawwa M.A., and Baroudi U., Effect of Leak Geometry on Water Characteristics Inside Pipes, *Sustainability* 14, 5224. (2022)
- [4]. De Sousa C. A. and Romero O. J., Influence of oil leakage in the pressure and flow rate behaviours in pipeline, *Latin American Journal of Energy Research*, 4, 17-29 (2017)
- [5]. De Sousa J. V. N., Sodre C. H. and De Lima A. G. B., Severino Rodrigues de Farias Neto (2013), Numerical Analysis of Heavy Oil-Water Flow and Leak Detection in Vertical Pipeline, *Advances in Chemical Engineering and Science*, 3, 9-15 (2013).
- [6]. Dubyk Y., Application of Probabilistic Leak-Before-Break for WWER-1000 Unit,” *Procedia Struct. Integr.*, 22, pp. 275–282, (2019).
- [7]. Ferreira da Silva I. G., Paes de Andrade A. H., and Monteiro W. A., Leak-Before-Break methodology applied to different piping materials: a performance evaluation, *Frattura ed Integrità Strutturale*, 50, pp. 46–53, (2019).
- [8]. Heckmann K., Elmas M. and Sievers J., Investigations on various leak types from operational experience and consequences for leak-before-break assessment of the pressure boundary, in *44th MPA-Seminar*, Stuttgart, Oct. 17–18, (2018).
- [9]. Kannan P., Amirthagadeswaran K.S. and Christopher T., Development and validation of a leak- before-break criteria for cylindrical pressure vessels, *Proc. Inst. Mech. Eng. Part L: J. Mater. Des. Appl.* 229(7), 636-646 (2015).
- [10]. Kebir T., Belhamiani M., Daikh A. A., Benguediab M., and Benachour M., “Investigating the effects of crack orientation and defects on pipeline fatigue life through finite element analysis,” *Fatigue of Aircraft Structures*, 2023, no. 15, pp. 1–21, (2023)
- [11]. Mansour M. A. B., Habib A., Khalifa A., Yousef Toumi K. and Chatzigeorgiou D., Computational fluid dynamic simulation of small leaks in water pipelines for direct leak pressure transduction, *Computers & Fluids* 57, 110-123 (2012)
- [12]. Ogunesan O. A., Hossain M., and Droubi M. G., Computational fluid dynamics modelling of multiphase flows in double elbow geometries, *Proc. IMechE, Part E: J. Process Mech. Eng.*, 235, no. 6, pp. 1835–1846, (2021).
- [13]. Roache P.J. and Annu., Quantification of uncertainty in computational fluid dynamics’, *Rev. Fluid. Mech.* 29: 123 – 60 (1997)
- [14]. Shao Yu, Yao Tian, Gong Jinzhe, Liu Jinjie, Zhang Tuqiao and Tingchao Yu, Impact of Main Pipe Flow Velocity on Leakage and Intrusion Flow: An Experimental Study, *Water*, 11, 118; (2019)
- [15]. Sun T. Z., Wei Y. J., and Wang C., Prediction of cryogenic cavitation around hydrofoil by an extensional Schnerr-Sauer cavitation model, *J. Phys.: Conf. Ser.*, 656, 012180, 2015.